A Compressed Sensing Based Design for Formation of Range-Doppler Maps

Jabran Akhtar and Karl Erik Olsen
Norwegian Defence Research Establishment (FFI)
Box 25, 2027 Kjeller, Norway
Email: jabran.akhtar@ffi.no, karl-erik.olsen@ffi.no

***Abstract*— Compressed sensing (CS) based reconstruction methods have been in much focus over the last years as they provide a mean to work with limited amount of data. In this article we present an application of CS and sparse reconstruction in a radar setup to form range-Doppler maps. We characterize a radar system where instead of transmitting a train of pulses the pulse transmission occurs in a sparse manner. An array based radar may thus for example alternate beams between two or more angles within the same processing interval applying the entire array. We show that gaps in data can very adequately be filled in by sparse reconstruction which can also be used to extrapolate additional values. Comprehensive simulations covering various scenarios, including sea clutter conditions, are used to demonstrate the effectiveness of the scheme.**

I. Introduction

Radar systems play an important role in air surveillance, detection and tracking of targets. A typical radar may operate by transmitting a number of pulses at a specific direction, stacking up returned matched filtered data in a matrix and performing a Fourier transform across the slow-time domain. This results in a range-Doppler map which can be used for for example target detection. Modern radars are typically equipped with electronically steering arrays and are able to digitally steer a beam instantaneously. When emitting pulses in a given direction a radar may desire to transmit a number of pulses in a different direction for various purposes, such as tracking, and then come back to the main angle to resume standard operation. The radar may also be interested in dividing its time, within the same coherent processing interval, between two, or more, scanning directions and for example only transmit all the pulses in the same angle if some unusual activity does show up. This type of beam switching with all array elements introduces a number of empty gaps in the slow-time domain and a range-Doppler profile has to be constructed with fewer pulses, resulting in less integration gain and lower Doppler resolution.

In this regard, an interesting question is to what extent empty data segments can be reconstructed or interpolated from available data, particularly for the purpose of a range-Doppler plot. This work investigates the performance of such a system and suggests a compressed sensing (CS) type of framework [1], [2], [3] with emphasis on the slow-time / Doppler domain. Several previous papers have considered various aspects of employing a CS scheme is a radar context [4], [5], [6], [7], though the explicit construction of a range-Doppler map has only been given limited attention. In contrast to for example [7], [8], [9] we do not assume that the radar emits specific modulated subpulses or even a continuous pulse of trains in the same direction and also do not infer that the sampling of incoming pulses is done in a sparse fashion. A standard matched filtering operation is rather carried out on a pulse to pulse basis. The presented concept emphasizes emission and reception of pulses in a sparse manner itself, freeing up valuable time at the radar to do other tasks such as multiple beam switching with little to no performance loss. Unlike most other papers e.g. [4], we also treat each range bin independently leading to an ensemble of one-dimensional problems with tractable partial Fourier matrices. It is demonstrated that this simplified process, with individual reconstruction for each range bin, still manages to provide substantial flexibility and improvement to a radar system.

The motivation for CS comes from the fact that a range-Doppler profile is likely to be sparse in nature. Each target typically occupies a few Doppler bins. Clutter, if present, though more diverse in nature, is still often likely to be concentrated to within a specific Doppler bin interval. As the overall contour is otherwise dominated by noise a sparse reconstruction strategy may be competent at compiling a profile where the missing data has been repleted.

In addition to interpolating missing values, another application of the method is to extrapolate data beyond the end points to extract additional slow-time data elements. This alone can be useful addition to a system as before proceeding with a Fourier transform across slow-time, a windowing function is often applied to smooth out measurements and reduce sidelobe levels; data collected at the beginning and end of the integration period is thus weighted down. An extrapolation can provide more substance in making maximum use of all available data and on its own incorporated as a software enhancement not requiring extensive system redesign.

II. Signal model

We consider a radar system where transmission and reception of N pulses takes place during a determined slow-time coherent interval. At each pulse repetition interval $p(t)$ is emitted and the incoming signal at slow-time u, $u = 1, 2, ..., N$, be described by

$$s(t,u) = \sum_n \sigma_n p(t-\Delta_n) e^{j\nu_{n,u}} + \tilde{w}(t) \tag{1}$$

Dette er en postprint-versjon / This is a postprint version.
DOI til publisert versjon / DOI to published version: 10.1109/RADAR.2016.7485322

where t is fast-time. σ_n are reflectivity levels of incoming echoes and targets while Δ_n is the signal delay associated with each reflector, we assume these values remain unaltered during the dwell period. $j = \sqrt{-1}$ and $e^{jv_{n,u}}$ is the experienced Doppler phase shift and for a constant velocity object typically modeled by

$$v_{n,u} = v_{n,u-1} + \frac{r_n \, 4\pi f_c}{c \, \text{PRF}}, \tag{2}$$

where r_n is the radial velocity of target n, f_c carrier frequency, PRF pulse repetition frequency and c speed of light. For convenience we can define $v_{n,0} = 0$.

After transmission of each waveform the radar samples any incoming pulse reflections and a matched filtering operation is carried out via the time-reversed and conjugated pulse $p^*(-t)$. The pulse compressed data can then be specified as

$$Y(t,u) = p^*(-t) * s(t,u) \tag{3}$$

where $*$ prescribes convolution in fast-time. In a practical setting the fast-time parameter will also be discrete, we denote this explicitly as

$$\mathbf{Y}(t_m,u) = Y(t_m\Delta t,u),\ t_m = 1,2,....,R \ \ \in \mathbb{C}^{N\times R} \tag{4}$$

given Δt as the resolution of the radar. $R\Delta t$ thus corresponds to the largest time-delay associated with the maximum unambiguous radar range.

For further processing $\mathbf{Y}(t_m,u)$ is typically multiplied in slow-time by a windowing function $\mathbf{w}(u) \in \mathbb{C}^{N\times 1}$ to yield $\mathbf{Y}_W(t_m,u) = \mathbf{w}(u)\mathbf{Y}(t_m,u) \in \mathbb{C}^{N\times R}$. Performing a Fourier transformation with respect to slow-time, over all discrete time-delays, or equivalently ranges, results in the range-Doppler map matrix:

$$\mathbf{D}(t_m,\omega) = \mathbf{F}\ \mathbf{Y}_W(t_m,u) \ \in \mathbb{C}^{N\times R}. \tag{5}$$

$\mathbf{F}$ is the discrete Fourier matrix of size $N \times N$, $\mathbf{F}_{k,l} = \exp(2\pi jkl/N)$ while the inverse discrete Fourier matrix is expressed by $\hat{\mathbf{F}} = \frac{1}{N}\mathbf{F}^*$ where * is the conjugation operator. Notice that the above process is independent for each range bin. ω can readily be converted into $[-v_{max}\ \ v_{max}]$ where $v_{max} = \frac{c\,\text{PRF}}{4f_c}$ is the maximum unambiguous velocity, with the resolution in Doppler space given by N, $\Delta\omega = \frac{2v_{max}}{N}$.

We assume that for whatever reason the radar does not transmit N pulses right after each other in the same direction rather the truncated $\tilde{\mathbf{Y}}(t_m,\tilde{u}) \in \mathbb{C}^{N-K\times R}$ only contains $N-K$ slow-time measurements, $\tilde{u} = 1,2,...,N-K$, collected arbitrary within the coherent interval of N pulses. A typical range-Doppler plot may now still be constructed by applying a Fourier matrix of size $N-K \times N-K$, however, as (2) is not satisfied, incoherent data can result in lower integration gain and spectral leakage.

The method of sparse reconstruction is to assemble an extended range-Doppler profile using a sparse reconstruction procedure and thus attempt to retain a high resolution in slow-time. In case of (2) each target is concentrated in velocity and the profile can be assumed to be sparse. The reconstructed solution should ideally approximate (2) for each target and maximize overall sparsity in Doppler. For this we define L to indicate the number of desired output entries in slow-time and assume $L \geq N$. The reconstructed profile in slow-time is denoted by $\hat{\mathbf{Y}}(t_m,\hat{u}) \in \mathbb{C}^{L\times R}$, $\hat{u} = 1,...,L$ and the range-Doppler map is

$$\hat{\mathbf{D}}(t_m,\hat{\omega}) = \hat{\mathbf{F}}\ \hat{\mathbf{w}}(\hat{u})\hat{\mathbf{Y}}(t_m,\hat{u}) \in \mathbb{C}^{L\times R} \tag{6}$$

where $\hat{\mathbf{F}}$ is an $L \times L$ Fourier matrix. We additionally define a binary selection matrix $\mathbf{M} \in \mathbb{B}^{N-K\times L}$ by taking an $L \times L$ identity matrix and removing respective rows for which no collected data is available. $\bar{\mathbf{w}}(\tilde{u})$ is formed by selecting a windowing function of L entries, $\hat{\mathbf{w}}(\hat{u}) \in \mathbb{C}^{L\times 1}$, and truncating it to $N-K$ values by excluding samples at positions where no collected data is available:

$$\bar{\mathbf{w}}(\tilde{u}) = \mathbf{M}\hat{\mathbf{w}}(\hat{u}) \ \in \mathbb{C}^{N-K\times 1}. \tag{7}$$

The reconstructed matrix should have the same set of data at measured positions:

$$(\mathbf{M}\hat{\mathbf{Y}})(t_m,\tilde{u}) = \tilde{\mathbf{Y}}(t_m,\tilde{u}), \tag{8}$$

or with windowing functions included

$$\mathbf{M}(\hat{\mathbf{w}}\hat{\mathbf{Y}})(t_m,\tilde{u}) = (\mathbf{M}\hat{\mathbf{w}})\tilde{\mathbf{Y}}(t_m,\tilde{u}). \tag{9}$$

This may be expressed as

$$(\mathbf{M}\hat{\mathbf{F}}^*\hat{\mathbf{F}}\hat{\mathbf{w}}\hat{\mathbf{Y}})\ (t_m,\tilde{u}) = \bar{\mathbf{w}}\tilde{\mathbf{Y}}\ (t_m,\tilde{u}) \tag{10}$$

leading to

$$\hat{\mathbf{F}}_R\hat{\mathbf{D}}\ (t_m,\hat{\omega}) = \bar{\mathbf{w}}\tilde{\mathbf{Y}}\ (t_m,\tilde{u}), \tag{11}$$

given the partial inverse Fourier matrix $\hat{\mathbf{F}}_R = \mathbf{M}\hat{\mathbf{F}}^* \in \mathbb{C}^{N-K\times L}$.

For a range $T = t_m$ the objective is therefore to determine a sparse Doppler profile $\hat{\mathbf{D}}(T,\hat{\omega})$ consisting of L samples while being in agreement with the observations. The reconstruction problem under convex relaxation therefore takes the shape of

$$\hat{\mathbf{D}}(T,\hat{\omega}) = \arg\min ||\dot{\mathbf{D}}(T,\hat{\omega})||_1 \tag{12}$$

under the constraint

$$||\ \hat{\mathbf{F}}_R\ \dot{\mathbf{D}}(T,\hat{\omega}) - \bar{\mathbf{w}}(\tilde{u})\ \tilde{\mathbf{Y}}(T,\tilde{u})\ ||\ \leq \delta \tag{13}$$

where δ is acceptable error limit while $||\ ||_1$ indicates the L1 norm.

Finding an independent solution over all defined values of $t_m = 1,2,....,R$ produces a range-Doppler map matrix $\hat{\mathbf{D}}(t_m,\hat{\omega}) \in \mathbb{C}^{L\times R}$ where any missing data would effectively have been inter- or extrapolated. In a practical setting the optimization processes may be run in parallel as each range bin poses a separate problem. δ may accordingly be set to the estimated noise level to restrict its influence or to a value relative to $||\bar{\mathbf{w}}(\tilde{u})\mathbf{Y}(T,\tilde{u})||$.

The design of $\hat{\mathbf{F}}_R$ can be selected randomly (e.g. random beam switching) or designed deterministically (e.g. predetermined beam switching pattern) where the matrix can be optimized beforehand to provide substantial high degree of recovery [1], [10], [11], [12], [13], [14].

Dette er en postprint-versjon / This is a postprint version.
DOI til publisert versjon / DOI to published version: 10.1109/RADAR.2016.7485322

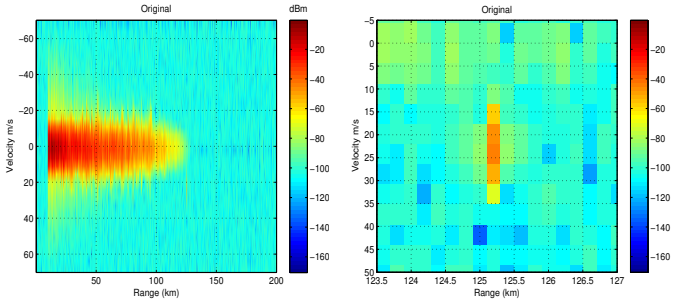

(a) Full (b) Zoomed in, $T_{max}: -44.15dBm$

Fig. 1: Original R-D map with 32 pulses

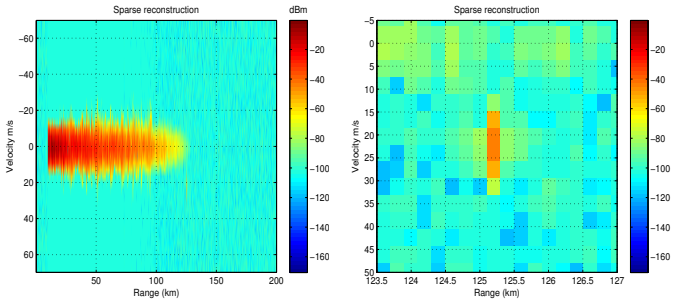

(a) Full (b) Zoomed in, $T_{max}: -43.02dBm$

Fig. 2: Sparse reconstruction, 3 extrapolations on both ends

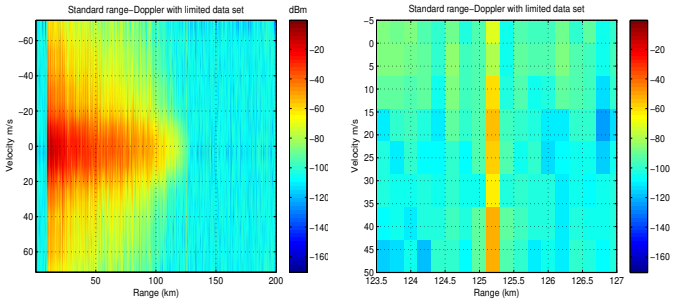

(a) Full (b) Zoomed in, $T_{max}: -50.98dBm$

Fig. 3: Standard R-D map with 20 random pulses (out of 32)

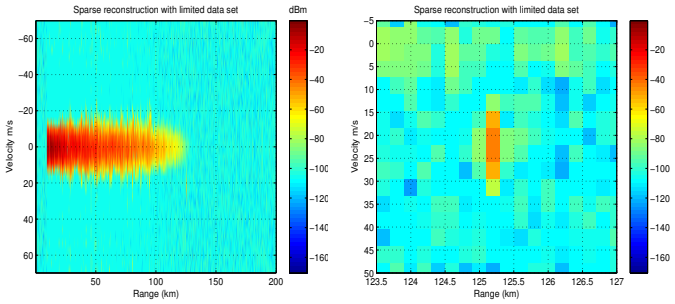

(a) Full (b) Zoomed in, $T_{max}: -43.02dBm$

Fig. 4: Reconstruction from 20 random pulses (6 extrapolations)

An artifact of sparse reconstruction is that $\hat{\mathbf{D}}$ may contain figures exactly identical to zero; making it difficult to compute signal to noise ratios. For displaying purposes, zero values may be set to the a priori estimated noise level, as done in this text.

III. Simulated data

In this section we review the performance of CS and seek restoration of range-Doppler maps with limited amount of available data. For this end we employ an in-house radar simulator which can simulate various target, clutter and noise conditions. The simulator uses Advanced Propagation Model (APM) [15] as propagation model and The Georgia Institute of Technology model (GIT) [16] for sea clutter modeling. Including sea clutter in a scenario presents for a more challenging and realistic environment while it also provides insight on a less sparse scene. For the simulation case the wind speed is set to 10m/s creating significant sea clutter conditions whose amplitude is modeled with an K-distribution and an Gaussian spectrum with mean 0 and slightly varying spread. A Swerling 1 target with radar cross section of $0.2m^2$ is simulated with velocity of 20m/s and altitude of 10m placed approximately 125km from the radar just outside the clutter region. The coherent period of target and clutter is assumed to correspond to 32 pulses. The radar antenna has beamwidths of 2°, altitude set at 1000m operating at 3GHz, a bandwidth of 0.8 MHz, emitting power at 15kwatt, antenna transmit and receive gain of 37dB and an PRF of 3000. The average noise figure evaluates to -107dBm and the Blackman window has been utilized throughout. The sparse solutions are found through a spectral projection gradient method with $\delta = 0.01||\bar{\mathbf{w}}(\tilde{u})\ \tilde{\mathbf{Y}}(T,\tilde{u})||$, i.e. an overall 1% deviation from the original values is permitted.

A. Extrapolation only

We first consider the case where the radar transmits all $N = 32$ pulses in the same direction and sparse reconstruction is solely used to extrapolate three additional values at both ends.

Figure 1 shows the original $N = 32$ pulse range-Doppler plot generated from simulated data where the target after processing attains an SNR of 48dB while figure 2 shows the outcome from extrapolated sparse reconstruction with a total of 6 extra ($L = 38$) Doppler bins. Extrapolation contributes with 1.1dB extra to the target power in this case while still retaining the target within four Doppler bins effectively improving the accuracy. The peak clutter power is likewise slightly increased but clutter is otherwise nicely joined together with reduced sidelobe levels and most of the spikes stand out as before.

B. Beam switching, 32 pulses

A more suggestive CS application of the method is to have alternating beams in a predefined time limit. The radar transmits a few pulses in one particular direction before transmitting a batch of pulses in another direction using the entire radar array. The radar iterates this a number of times within the coherent processing interval till a desired number of pulses have been collected. Sparse reconstruction can then be used to fill in gaps and to maintain comparable resolution in Doppler as if all pulses had been emitted in this direction. The transmission pattern can in a typical CS framework

Dette er en postprint-versjon / This is a postprint version.
DOI til publisert versjon / DOI to published version: 10.1109/RADAR.2016.7485322

be designed in a random or pseudo-random manner with a specific ratio between the various scan angles and to minimize mutual coherence of matrices. [17], [18], [11], [19].

An example of the results obtained is demonstrated next where the radar only transmits $N - K = 20$ pulses, out of standard $N = 32$, in a random order, at the main direction. Figure 3 shows the outcomes in the case of standard pulse-Doppler processing where the Doppler resolution is quite low due to the decreased number of slow-time data. The target is dimmer with spectral leakage. The results from sparse reconstruction with the identical data set given in figure 4 show a somewhat different picture. The target still stands out quite clear with a comparable power level and still preserving good accuracy in Doppler. The sea clutter pattern is also continuous and generally well-behaved much in line with figure 2 but with the addition of minor low energy peaks at potential ambiguous Doppler velocities. Nevertheless, in an environment with less clutter this is unlikely to be of any major concern.

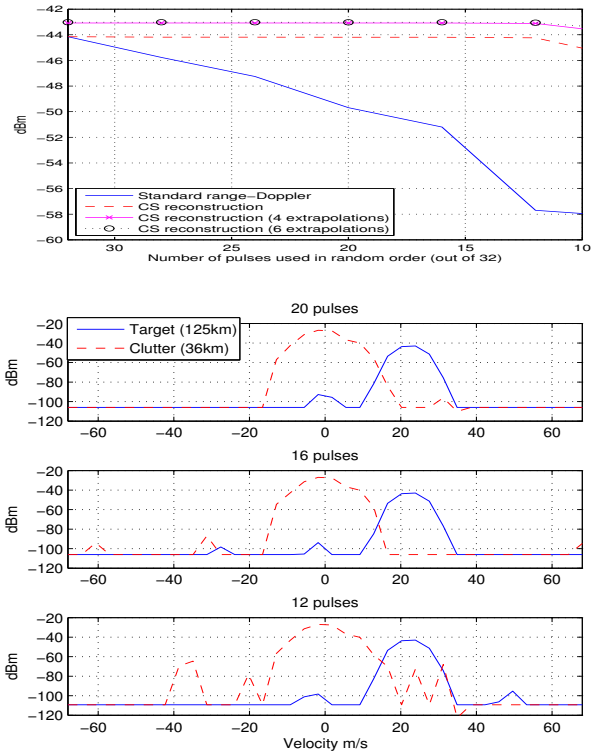

Fig. 6: Reconstructed target and clutter Doppler profiles

Figure 5 shows a more comprehensive graph over how the average peak target energy varies with varying number of available pulses and sparse reconstruction with or without extrapolation alongside standard range-Doppler processing over 100 runs. As evident, sparse reconstruction is able to retain the target power level till a minimum of about $N = 12$ pulses and must be said to work exceptionally well for single targets. Extrapolating enriches with integration gain and the effect is sustained throughout.

Further on, figure 6 displays some examples of reproduced Doppler profiles for target and clutter at 36km with various

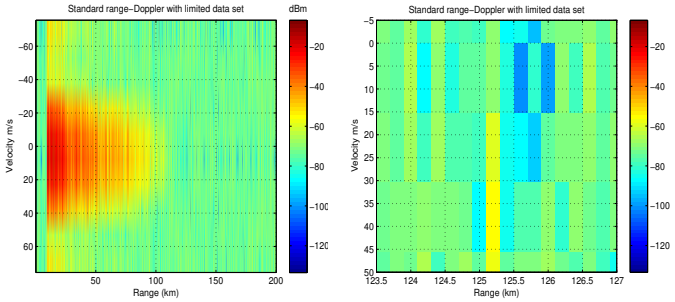

(a) Full (b) Zoomed in, $T_{max}: -55.28dBm$

Fig. 7: Standard R-D map with 10 random pulses (out of 16)

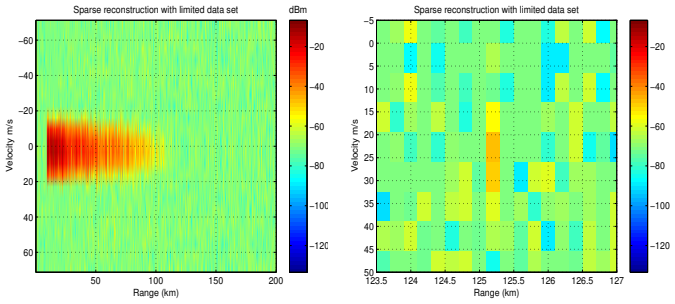

(a) Full (b) Zoomed in, $T_{max}: -48.32dBm$

Fig. 8: Reconstruction from 10 random pulses (6 extrapolations)

number of pulses and assuming 3 additional extrapolations on each end. Although the target stands out, clutter reconstruction starts to degrade when less than half of all pulses are available for reassembly.

C. Beam switching, 16 pulses and low SNR

In this subsection we rely on the same scenario as described previously but reduce the processing interval to $N = 16$ pulses. Noise is also greatly scaled up bringing the target SNR after standard Doppler processing to 17.6dB. Random pulse emission and reception thus occurs within a shorter time frame where fewer pulses will bring the SNR down even further. Figure 7 visualizes the obtained range-Doppler map in the case of $N - K = 10$ pulses while figures 8 and 9, respectively, show the reconstructed plots with $L = 22$ (3 extrapolations on each side) and $L = 32$ (8 extrapolations on

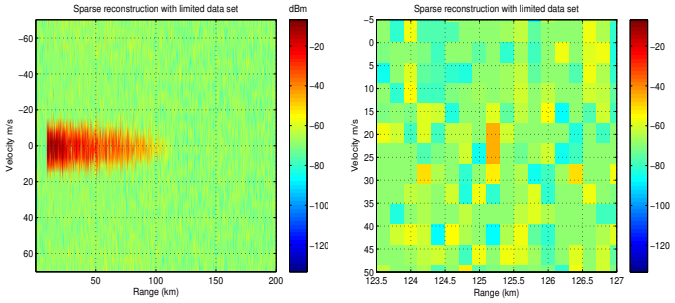

(a) Full (b) Zoomed in, $T_{max}: -44.75dBm$

Fig. 9: Reconstruction from 10 random pulses (16 extrapolations)

Dette er en postprint-versjon / This is a postprint version.
DOI til publisert versjon / DOI to published version: 10.1109/RADAR.2016.7485322

each side). The difference between the results obtained via standard Fourier processing and CS is quite noticeable with over 7dB difference in observed target power ($L = 22$) while additional extrapolation increases this further.

Figure 10 shows average peak target energy levels for different number of pulses over 100 runs. The performance of sparse reconstruction for the main target starts to suffer when the number of available pulses approximately reaches one half which is also verifiable via the Doppler profiles in figure 11.

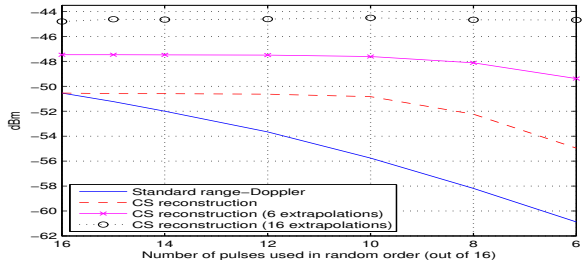

Fig. 10: Average peak target energy

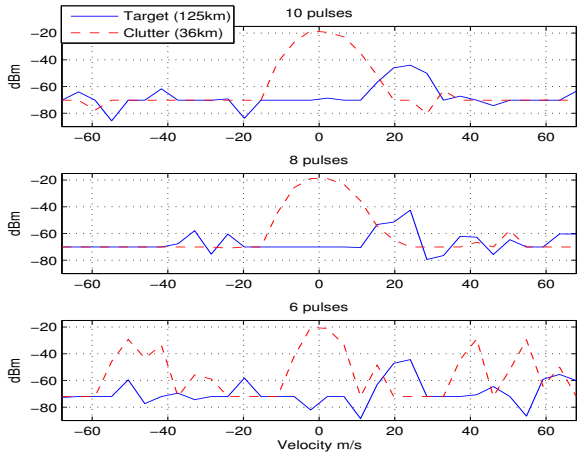

Fig. 11: Reconstructed target and clutter Doppler profiles with varying number of available pulses (out of 16) and 16 extrapolations

The random pulse emission method utilized for the simulations can most likely be improved upon by optimizing the transmission structure [14]. In any case, formation through sparse reconstruction expands upon what is typically attainable through standard Doppler processing for the same amount of data.

IV. Conclusion

The use of compressed sensing based techniques for construction of range-Doppler maps has been considered. The emphasis of this work was on the slow-time domain under a standard radar employing matched filter processing on each single pulse. CS can permit a radar to emit pulses in a sparse manner freeing up valuable time at the radar. It was shown that sparse reconstruction methods can be exploited to fill in missing values and the same approach can also be used to extrapolate supplementary figures at the beginning and end of a data set. The results indicate that sparse reconstruction, with independent optimization for each range bin, performs well and quality maps can be obtained, even in the presence of energetic clutter, with reduced amount of radar data.

V. Acknowledgments

The authors would like to thank Dr. Terje Johnsen for aiding with the radar simulator.

References

[1] E. Candes, J. Romberg, and T. Tao, "Stable signal receovery from incomplete and inaccurate measurments," *Communication in Pure and Applied Mathematics*, vol. 59, pp. 1207–1223, 2006.

[2] L. C. Potter, E. Ertin, J. T. Parker, and M. Cetin, "Sparsity and compressed sensing in radar imaging," *Proceedings of the IEEE*, vol. 98, no. 6, pp. 1006–1020, 2010.

[3] M. F. Durate and Y. C. Eldar, "Structured compressed sensing: From theory to applications," *IEEE Transactions on Signal Processing*, vol. 59, pp. 4053–4085, 2011.

[4] M. A. Herman and T. Strohmer, "High-resolution radar via compressed sensing," *IEEE Trans. Signal Processing*, vol. 57, no. 6, pp. 2275–2284, June 2009.

[5] M. Amin, F. Ahmad, and Z. Wenji, "A compressive sensing approach to moving target indication for urban sensing," in *IEEE Radar Conference*, 2011, pp. 509–511.

[6] R. A. Sevimli, M. Tofighi, and A. E. Cetin, "Range-doppler radar target detection using denoising within the compressive sensing framework," in *European Signal Processing Conference*, 2014, pp. 1950–1954.

[7] B. Pollock and N. A. Goodman, "Detection performance of compressively sampled radar signals," in *IEEE Radar Conference*, 2011, pp. 1117–1122.

[8] T. Xing, W. Roberts, L. Jian, and P. Stoica, "Range-doppler imaging via a train of probing pulses," *IEEE Trans. Signal Processing*, vol. 57, no. 3, pp. 1084–1097, March 2009.

[9] M. M. Hyder and K. Mahata, "Range-doppler imaging via sparse representation," in *IEEE Radar Conference*, 2011, pp. 486–491.

[10] M. Fornasier and H. Rauhut, *"Compressive sensing" in "Handbook of mathematical methods in imaging" O. Scherzer (Eds.)*. Springer New York, 2011.

[11] N. Y. Yu and Y. Li, "Deterministic construction of Fourier-based compressed sensing matrices using an almost difference set," *EURASIP Journal on Advances in Signal Processing*, vol. 155, pp. 805–821, Oct. 2013.

[12] D. S. Kalogerias and A. P. Petropulu, "RIP bounds for naively subsampled scrambled Fourier sensing matrices," in *Conference on Information Sciences and Systems*, 2014, pp. 1–6.

[13] B. Adcock, A. C. Hansen, C. Poon, and B. Roman, "Breaking the coherence barrier: asymptotic incoherence and asymptotic sparsity in compressed sensing," in *International Conference on Sampling Theory and Applications*, July 2013.

[14] G. Xu and Z. Xu, "Compressed sensing matrices from Fourier matrices," *IEEE Trans. Inf. Theory*, vol. 61, no. 1, pp. 469–478, Jan. 2015.

[15] A. E. Barrios, "Considerations in the development of the advanced propagation model (APM) for U.S. Navy applications," in *IEEE Radar Conference*, 2003, pp. 77–82.

[16] M. M. Horst, F. B. Dyer, and M. Tuley, "Radar sea clutter model," in *Proc. of the Intl. IEEE AP/S URSI Symposium*, 1978, pp. 6–10.

[17] X. Bian and N. Y. Yu, "Partial Fourier codebooks associated with multiplied golay complementary sequences for compressed sensing," in *Intl. Conference on Sequences and Their Applications*, 2012, pp. 257–268.

[18] N. Y. Yu, "On statistical restricted isometry property of a new class of deterministic partial Fourier compressed sensing matrices," in *Intl. Symposium on Information Theory and its Applications*, 2012, pp. 284–288.

[19] J. Ma, X. Yuan, and L. Ping, "Turbo compressed sensing with partial DFT sensing matrix," *IEEE Signal Processing Letters*, vol. 22, pp. 158–161, feb 2015.